

# Accepted Manuscript

Synthesis and biological evaluation of new water-soluble photoactive chlorin conjugate for targeted delivery

Vasilii F. Otvagin, Alexander V. Nyuchev, Natalia S. Kuzmina, Ivan D. Grishin, Andrei E. Gavryushin, Yuliya V. Romanenko, Oscar I. Koifman, Dmitrii V. Belykh, Nina N. Peskova, Natalia Yu Shilyagina, Irina V. Balalaeva, Alexey Yu. Fedorov

PII: S0223-5234(17)31094-2

DOI: [10.1016/j.ejmech.2017.12.062](https://doi.org/10.1016/j.ejmech.2017.12.062)

Reference: EJMECH 10040

To appear in: *European Journal of Medicinal Chemistry*

Received Date: 11 August 2017

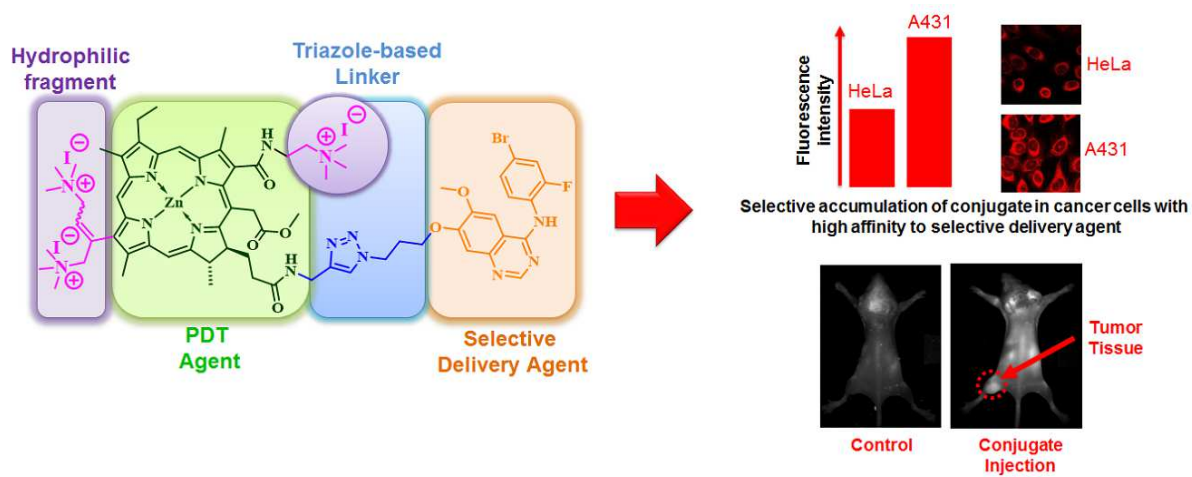
Revised Date: 15 December 2017

Accepted Date: 16 December 2017

Please cite this article as: V.F. Otvagin, A.V. Nyuchev, N.S. Kuzmina, I.D. Grishin, A.E. Gavryushin, Y.V. Romanenko, O.I. Koifman, D.V. Belykh, N.N. Peskova, N.Y. Shilyagina, I.V. Balalaeva, A.Y. Fedorov, Synthesis and biological evaluation of new water-soluble photoactive chlorin conjugate for targeted delivery, *European Journal of Medicinal Chemistry* (2018), doi: 10.1016/j.ejmech.2017.12.062.

This is a PDF file of an unedited manuscript that has been accepted for publication. As a service to our customers we are providing this early version of the manuscript. The manuscript will undergo copyediting, typesetting, and review of the resulting proof before it is published in its final form. Please note that during the production process errors may be discovered which could affect the content, and all legal disclaimers that apply to the journal pertain.





## Chlorin Conjugate for Targeted Delivery

Vasilii F. Otvagin<sup>a</sup>, Alexander V. Nyuchev<sup>a</sup>, Natalia S. Kuzmina<sup>a</sup>, Ivan D. Grishin<sup>a</sup>, Andrei E. Gavryushin<sup>b</sup>, Yuliya V. Romanenko<sup>c</sup>, Oscar I. Koifman<sup>c</sup>, Dmitrii V. Belykh<sup>d</sup>, Nina N. Peskova<sup>a</sup>, Natalia Yu. Shilyagina<sup>a</sup>, Irina V. Balalaeva<sup>a,e\*</sup>, Alexey Yu. Fedorov<sup>a\*</sup>

<sup>a</sup>Lobachevsky State University of Nizhny Novgorod, Gagarina av. 23, Nizhny Novgorod 603950, Russian Federation, Fax: +7 831-462-30-85, E-mail: [afnn@rambler.ru](mailto:afnn@rambler.ru)

<sup>b</sup>Ludwig-Maximilians-Universität, Butenandtstrasse 5-13, 81377, Munich, Germany

<sup>c</sup>Research Institute of Macroheterocycles, Ivanovo State University of Chemical Technology, 153000 Ivanovo, Russian Federation

<sup>d</sup>Institute of Chemistry, Komi Scientific Center, Urals Branch of the Russian Academy of Sciences, 167982 Syktyvkar, Russian Federation

<sup>e</sup>Sechenov First Moscow State Medical University, Trubetskaya str. 8-2, Moscow 119991, Russian Federation

\*Corresponding authors

Prof. Alexey Yu. Fedorov

<sup>a</sup>Lobachevsky State University of Nizhny Novgorod, Gagarina av. 23, Nizhny Novgorod 603950, Russian Federation, Fax: +7 831-462-30-85, E-mail: [afnn@rambler.ru](mailto:afnn@rambler.ru)

Dr. Irina V. Balalaeva

<sup>a</sup>Lobachevsky State University of Nizhny Novgorod, Gagarina av. 23, Nizhny Novgorod 603950, Russian Federation, Tel/Fax +7 831-462-32-13, E-mail: [irin-b@mail.ru](mailto:irin-b@mail.ru)

**Keywords:** chlorins, conjugate, PDT, targeted delivery, water-solubility, medicinal chemistry.

## Abstract

A new water-soluble conjugate, consisting of a chlorin-based photosensitizing part, and a 4-arylaminoquinazoline moiety with high potential affinity to an epidermal growth factor receptors (EGFR) and vascular endothelial growth factor receptors (VEGFR), suitable for photodynamic therapy (PDT), was synthesized starting from methylpheophorbide-*a* in seven steps. An increased accumulation of this compound in A431 cells with high level of EGFR expression, in comparison with CHO and HeLa cells with low EGFR expression was observed. The prepared conjugate exhibits dark and photoinduced cytotoxicity at micromolar concentrations with  $IC_{50\text{dark}}/IC_{50\text{light}}$  ratio of 11-18. In tumor-bearing mice, the conjugate preferentially accumulates in the tumor tissue.

## 1. Introduction

Photodynamic therapy (PDT) is a clinically approved low-invasive procedure for the treatment of oncological and dermatological diseases as well as an efficient method for therapy of fungal, viral and bacterial infections [1-5]. The therapeutic effect of PDT in the targeted tissue is based on photochemical conversion of oxygen by a preactivated by light photosensitizer (PS), leading to the generation of singlet oxygen or active radical particles, known as reactive oxygen species (ROS) [6,7]. Such species, in turn, are able to induce cellular damage in the areas proximal to the PS localization. PDT method is well-established in the treatment of superficial tumors, such as skin, head and neck cancer, as well as tumors of hollow viscera, in particular, oral tumors, esophagus, stomach, colon, lung, breast, cervix, prostate, and bladder cancer [1a, 1b]. Among the obstacles for wider application of PDT is the low selectivity of the PS accumulation in tumor tissues. The accumulation of a

photosensitizer in skin and mucous membranes leads to undesirable side effects such as phototoxicity. A way to regulate the biodistribution of a photosensitizer and thus improve its overall efficiency upon systemic administration is the application of carrier-linked drug delivery [8]. The conjugation of a biologically active agent with macromolecules such as antibodies, polysaccharides, lectins, serum proteins, peptides, growth factors and synthetic polymers, as well as its incorporation into micelles or liposomes can dramatically change its biodistribution and enhance its therapeutic potential [9].

The idea behind this work is the development of potentially therapeutically useful conjugates which would (a) act as both PDT-photosensitizers and cytotoxic agents; (b) selectively accumulate in tumor cells; (c) allow the fluorescence imaging of their tissue distribution; (d) possess acceptable physical properties such as water solubility (Figure 1). Theranostic agents for the simultaneous imaging and targeted non-invasive treatment of cancer have become of increasing interest over the last decade [10].

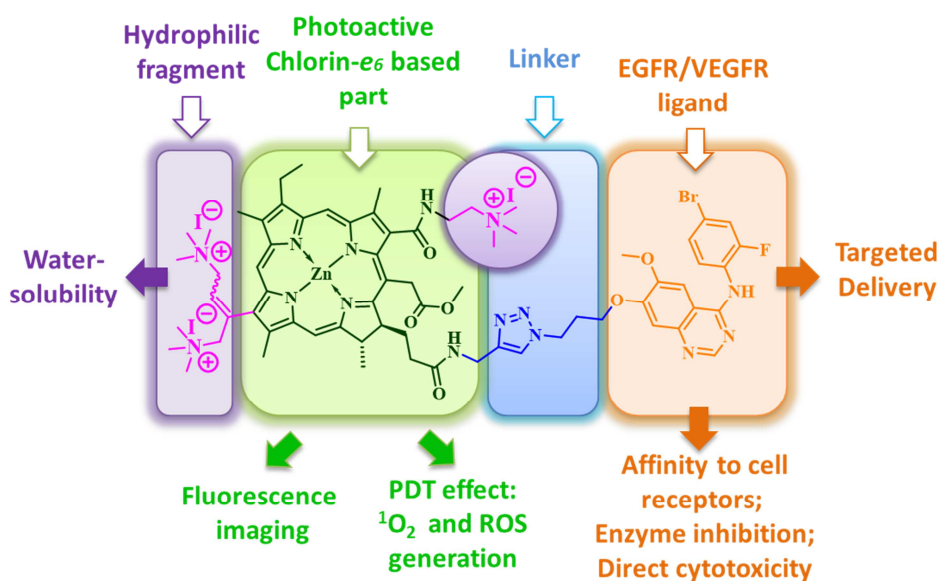


**Figure 1.** Structure of a proposed conjugate.

A number of synthetic or semi-synthetic chlorins (NPe6, Foscan, Fotolon, Photoditasine, and Tookad – a palladium bacteriopheophorbide PS, related to chlorins) are already used as photosensitizers in clinics [11-15]. Chlorin- $e_6$  derivatives (Figure 2), belonging to the natural

metabolites of chlorophyll *a*, are prone to simple chemical functionalization, exhibit strong fluorescence in the red part of the visible spectrum and display good quantum yield of singlet oxygen and ROS production [16]. Owing to the presence of three carboxyl groups, these compounds are relatively hydrophilic [17]. At the same time, chlorin-*e*<sub>6</sub> derivatives manifest amphiphilic properties, since the carboxyl groups are placed on the same side of the heterocyclic core. Due to their pronounced photocytotoxicity, chlorin-*e*<sub>6</sub> (Photolon) or its derivatives (Radachlorin or Photoditasine) are used for the treatment of sarcoma and brain cancers [18]. A less hydrophilic benzochlorin Verteporfin (trade name Visudyne) is used in UK for the treatment of ophthalmic, pancreatic and skin cancer [18b]. The attachment of L-aspartic acid moiety to the chlorin core increases the hydrophilicity of the molecule giving compound known as Talaporfin (or NPe6) – mono-L-aspartyl chlorin-*e*<sub>6</sub>. It is less photocytotoxic than the parent compound, and has been approved in USA for cure of liver, colon and brain cancers [18b]. Completely synthetic and highly hydrophilic Temoporfin (Foscan) is also used for the treatment of these types of cancer.

The incorporation of a non-transition metal into the chlorin core can influence the balance between the quantum yields of singlet oxygen and the compound fluorescence. So, the complexation of chlorin-*e*<sub>6</sub> with Sn(IV) increases the singlet oxygen yield. This effect was used in the development of SnEt<sub>2</sub>/Purlytin, the drug used for the treatment of the skin and breast cancers [18]. The complexation with zinc leads to a drop of the singlet oxygen yield, with a simultaneous increase in the fluorescence quantum yield. The incorporation of paramagnetic metals completely inhibit <sup>3</sup>O<sub>2</sub> production [17].

The PS aggregation can profoundly influence the efficiency of a compound for PDT therapy. Chlorin-*e*<sub>6</sub> itself is monomeric in the aqueous solutions. However,  $\pi$ - $\pi$  stacking and hydrophobic interactions between the molecules of chlorin-*e*<sub>6</sub> derivatives might cause their self-aggregation and thus a harsh drop of the ROS generation *via* self-quenching [19]. Extensive aggregation along with poor accumulation of chlorins in the tumor tissues, and

long-lasting phototoxicity for healthy tissues are the major problems preventing broader use of chlorin-*e*<sub>6</sub> PSs [20].

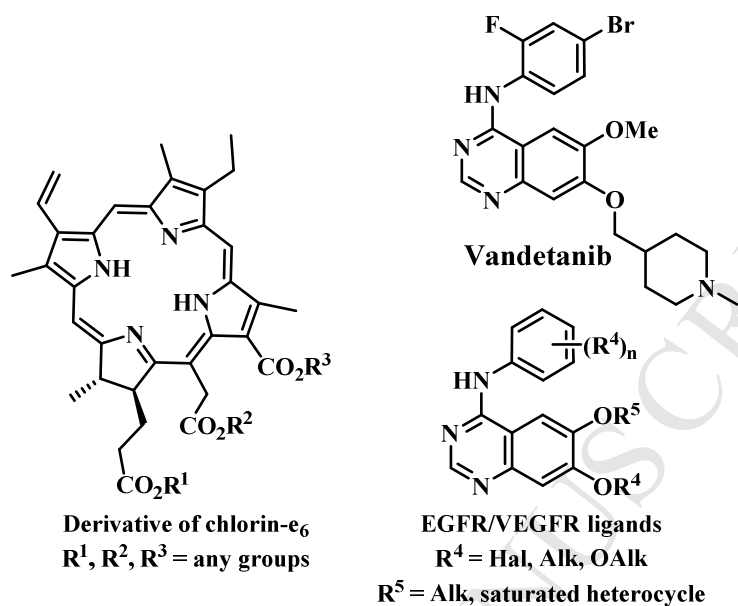


**Fig.2.** Chlorin-type photosensitizers and epidermal growth factor receptor (EGFR)/vascular endothelial growth factor receptor (VEGFR) ligands.

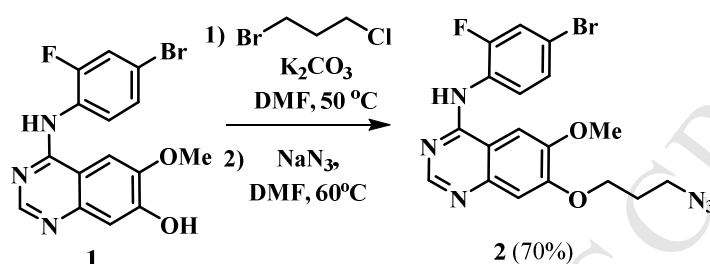
To improve the selectivity of PS accumulation in the tumor tissue, we performed the conjugation of the chlorin core with 4-arylaminoquinazolines (Figure 2) belonging to a family of high affinity ligands of epidermal growth factor and vascular endothelial growth factor receptors ((EGFR and VEGFR). Such receptors are often highly expressed by rapidly growing tumor tissues, due to the necessity to develop their own vasculature [21]. Substituted 4-arylaminoquinazolines such as Vandetanib (Figure 2, approved in 2011 by FDA for the treatment of late-stage medullary thyroid cancer) bind to these types of receptors, inhibiting their tyrosine kinase activity [22].

In order to improve water solubility of the target conjugates [23], we attached hydrophilic tetraalkylammonium moieties to the chlorin core of the molecule.

## 2. Results and discussion

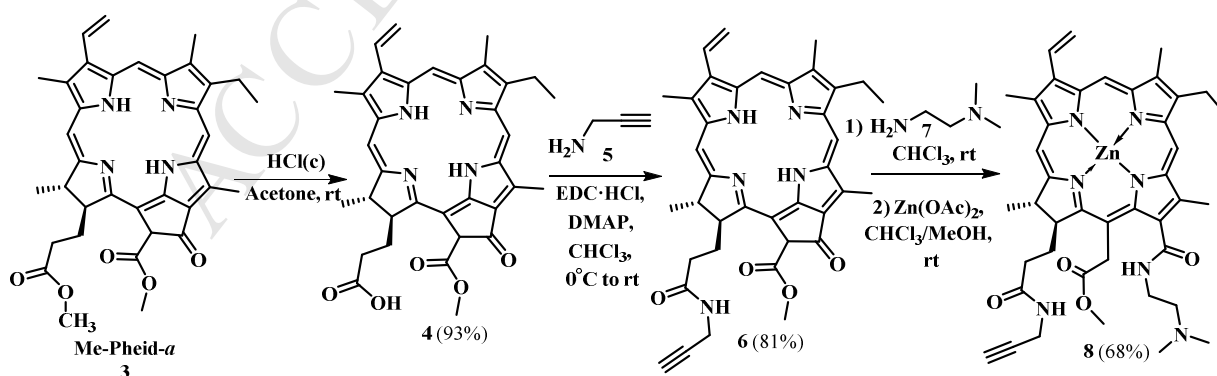
## Chemistry

The substituted 4-arylaminoquinazoline **1** was synthesized from vanillic acid according to the known procedure [24], and was converted into azido-ether **2** via two-step sequence (Scheme 1).



**Scheme 1.** Synthesis of azido-functionalized derivative **2**.

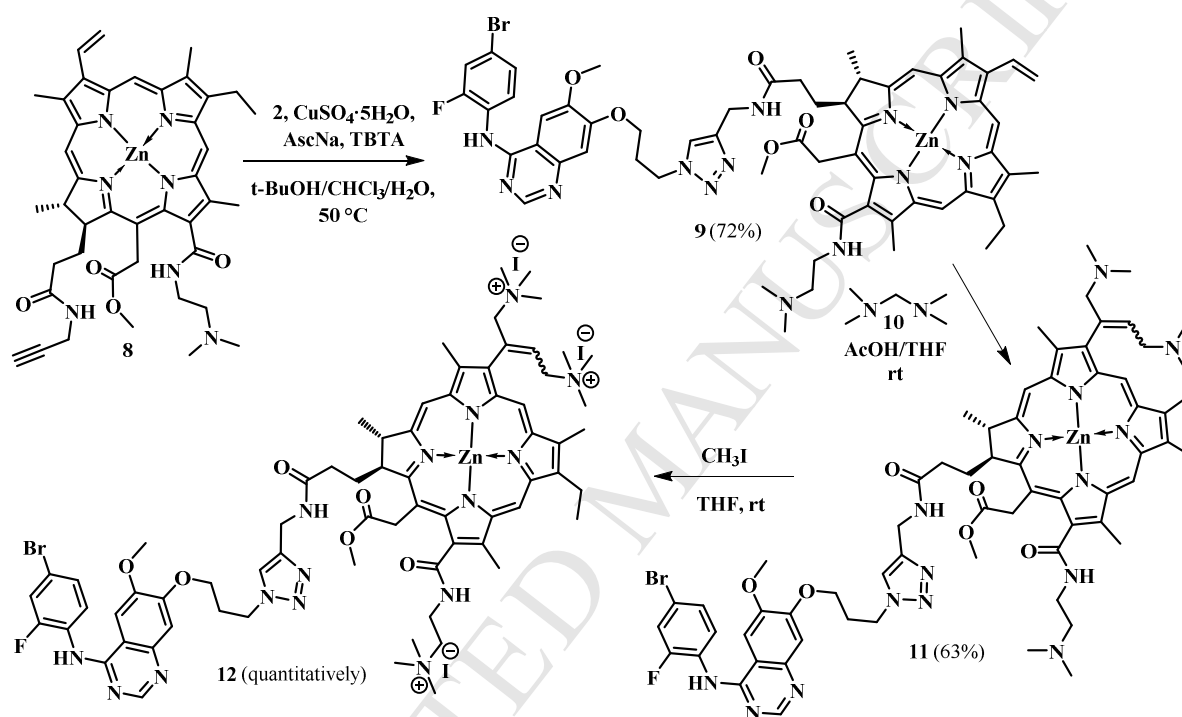
The photoactive parts of the conjugates were prepared from naturally occurring methylpheophorbide-*a* (**3**) (Scheme 2) [25]. At the first step, one of the two ester groups in **3** was selectively cleaved under the acidic conditions to afford acid **4** in 93% yield (Scheme 2). Its amidation with propargylamine according to the Steglich protocol [26] gave terminal alkyne **6**, isolated in 81% yield. It was subjected to a nucleophilic ring-opening [27] by the treatment with an excess of amine **7**. Zinc insertion in the next step afforded compound **8** in 68% yield.



**Scheme 2.** Synthesis of alkyne-functionalized chlorin-*e*<sub>6</sub> derivative.

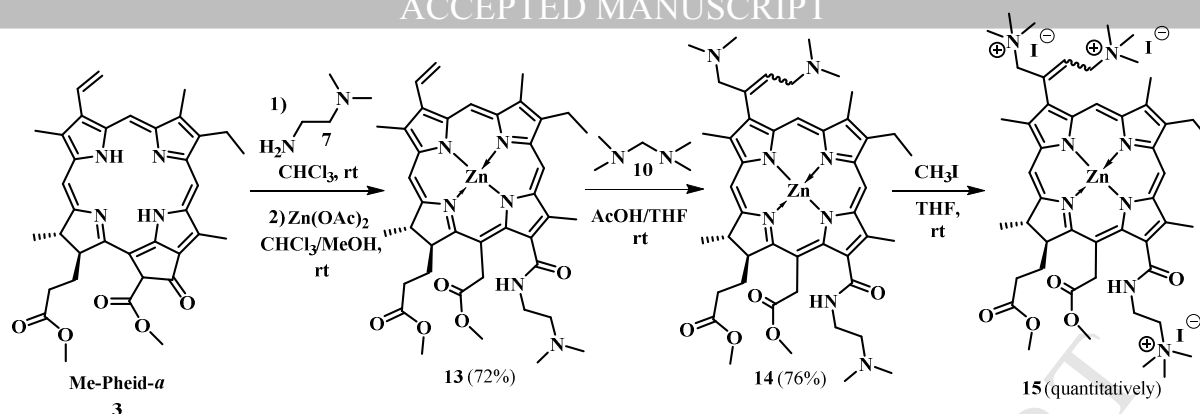
At the next step, alkyne **8** was subjected to the [3+2]-cycloaddition conjugation with azide **2** in the presence of CuSO<sub>4</sub>/AscNa/TBTA catalytic system in *t*-BuOH/CHCl<sub>3</sub>/H<sub>2</sub>O mixture [28]

that afforded conjugate **9** in 72% yield (Scheme 3). To increase its water solubility, chlorin **9** was aminomethylated by *bis*(dimethylamino)methane **10** via the *in situ* formation of the Eschenmoser salt, that proceeded at the peripheral vinyl fragment of the chlorin core [29]. The target conjugate **11**, bearing three tertiary amino groups was isolated in 63% yield. Finally, the quaternization of chlorin **11** with methyl iodide afforded quantitatively water-soluble and stable conjugate **12** (Scheme 3).



### Scheme 3. Synthesis of conjugate **12**.

In order to investigate the contribution of the quinazoline fragment to the antitumor activity and photophysical properties of conjugate **12**, a water-soluble chlorin **15** without EGFR/VEGFR ligand part was prepared in four steps starting from methylpheophorbide-*a* (Scheme 4).



**Scheme 4.** Synthesis of water-soluble chlorin-*e*<sub>6</sub> derivative without EGFR/VEGFR ligand.

The nucleophilic ring opening of the five-membered exocycle in methylpheophorbide-*a* **3** using amine **7** followed by the zinc insertion gave chlorin **13** in 72% yield. Its further aminomethylation with *bis*(dimethylamino)methane **10** afforded triamine **14** in 76% yield, which after quaternization gave water-soluble salt **15**.

The tetraalkylammonium salts **12** and **15** demonstrated desired solubility in water (~ 0.01 mol/L).

### Photophysical properties

Compounds **12** and **15** possess absorption spectra, characteristic for chlorins, with intense Soret and Q-bands at ~410 nm and ~630 nm, respectively (Table 1, Figure 3). These bands exhibit high molar absorptivities ( $\log \epsilon$  higher than 4.3), with higher values for the short-wave than for the long-wave region, also typical for chlorin dyes [30].

**Table 1.** Photophysical characterization of compounds **12** and **15** in water.

Compound	$\lambda_{\text{abs}}(\text{nm})$ ( $\log \epsilon$ )	$\lambda_{\text{em}}(\text{nm})^{\text{a}}$	$\Phi_{\text{F}}^{\text{b}}(\%)$
<b>12</b>	412 (4.80)	638	7.3
	632 (4.39)		
<b>15</b>	408 (4.96)	636	9.5
	628 (4.44)		

<sup>a</sup>Exited at 410 nm. <sup>b</sup>Relative to Rhodamine B in water.

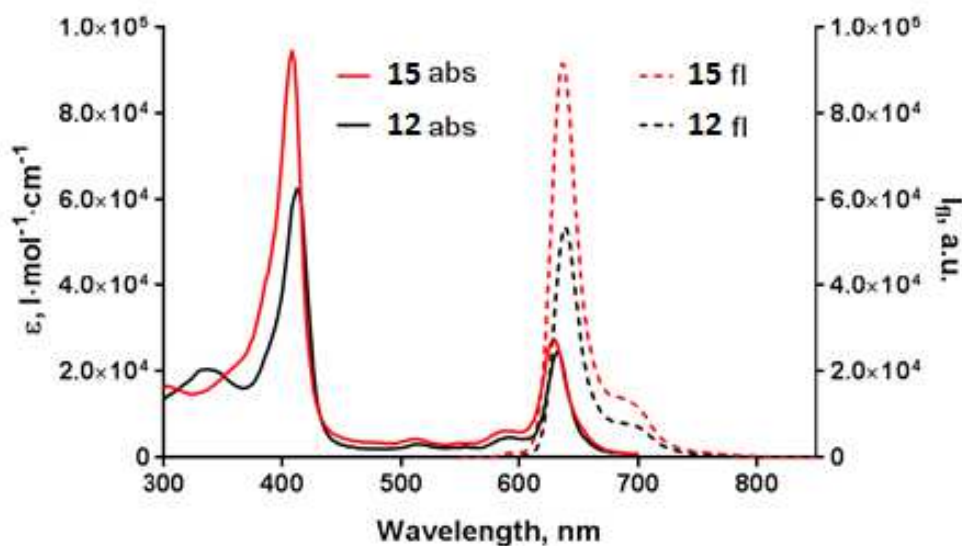


**Fig. 3.** Absorption and fluorescence spectra of **12** and **15** (both at 5  $\mu\text{M}$ ) in water.

Fluorescence was excited at 410 nm.

Both compounds manifested fluorescence in water with the maxima in red region ( $\sim 640$  nm) with the relative quantum yields (Rhodamine 6G) of 7.3% and 9.5% for **12** and **15**, respectively. Conjugate **12** demonstrated lower fluorescence than free photosensitizer **15**, what can be attributed to the partial quenching by the arylquinazoline part of the molecule.

## Biology

### *Cellular uptake*

The ability of the synthesized compounds **12** and **15** to penetrate and accumulate in living cells was studied on cell lines with various expression levels of epidermal growth factor receptor (EGFR): EGFR-negative CHO (chinese hamster ovary cells) [31], HeLa (human cervical carcinoma) [32] and A431 (human epidermoid carcinoma) [33]. All the chosen cell lines have minimal or negligible expression of VEGFR1 (Flt-1) and VEGFR2 (KDR/Flk-1) [34].

To quantify the relative level of EGFR expression, the cells were stained by anti-EGFR antibodies labeled with phycoerythrin (PE) and analyzed using flow cytometry (Figure 4).

HeLa cells demonstrated low level of EGFR-expression, with moderate staining by anti-EGFR antibodies (ca. 7-fold increase in the fluorescence signal to CHO-cells). On the contrary, A431 cells reveal high level of EGFR expression (fluorescence signal increased by two orders of magnitude after the labeling).

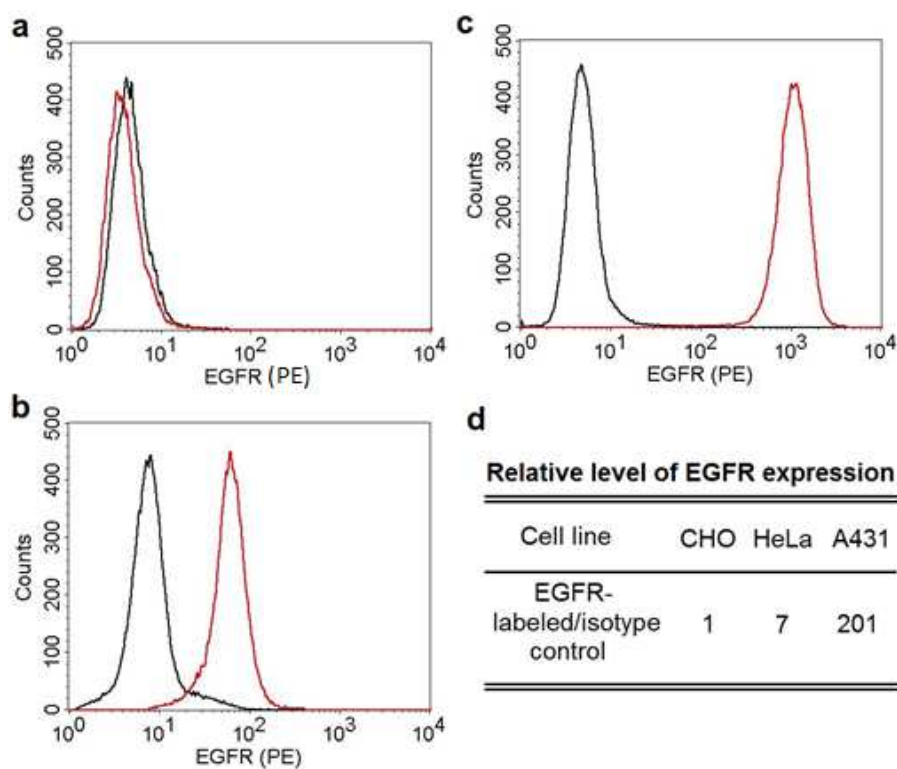


**Fig. 4.** Flow cytometry analysis of EGFR expression by cells of CHO (a), HeLa (b) and A431 (c) lines. Cells were stained with PE-labeled anti-EGFR antibodies (red) or isotype control (black) and their fluorescence ( $\lambda_{\text{ex}}$  488 nm,  $\lambda_{\text{em}}$  564-606) was measured by FACS. The distribution of 30 000 cells depending on PE fluorescence intensity is shown. (d) Relative level of EGFR expression was calculated from flow cytometry data as the ratio of geometric mean fluorescence intensities in EGFR-labeled and isotype control cells.

When conjugate **12** was incubated with CHO, HeLa and A431 cells during 4 hours, an increased accumulation of this compound in A431 cells was observed (**Figure 5**). The cellular uptake of **12** in CHO and HeLa cells was significantly lower. Thus, the conjugate **12**, containing arylaminoquinazoline vector to EGFR, preferentially accumulates in the cells with high expression of such receptors. We presume, however, that both non-specific and EGFR-

facilitated mechanisms contribute comparably to the conjugate **12** internalization in HeLa cells. Interestingly, compound **15** accumulates in the cells of all three lines (CHO, HeLa and A431) at a significantly lower level.

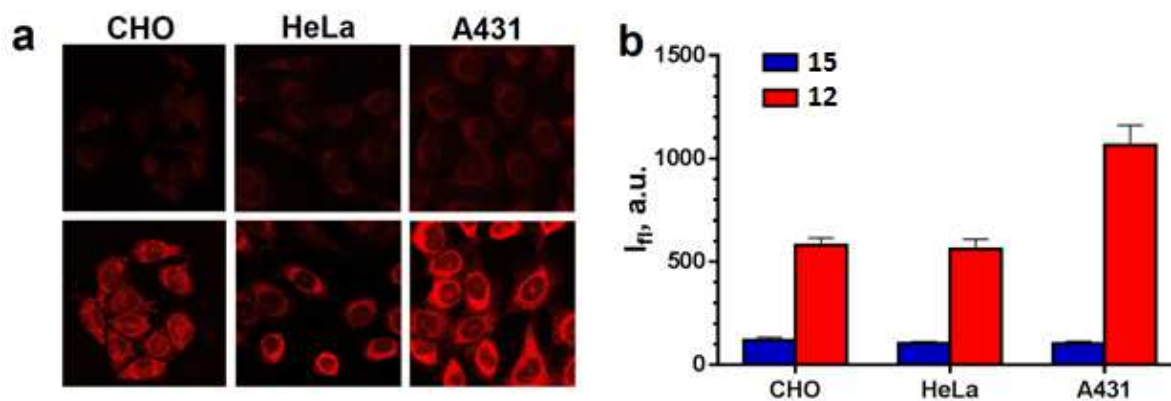


**Fig. 5.** (a) Confocal images on CHO, HeLa and A431 cells after incubation with 5  $\mu$ M for 4h, conjugate **12** (bottom line), compound **15** (top line).  $\lambda_{ex}$  405 nm,  $\lambda_{em}$  600–740 nm. Images size 143  $\mu$ m  $\times$  143  $\mu$ m. (b) Comparison of the corresponding intracellular fluorescence intensity for **12** and **15**. At least ten cells in two-three fields of view were analyzed; mean  $\pm$  SEM are presented.

#### *Dark and photoinduced cytotoxicity*

A standard MTT-assay was used to determine the concentration of **12** and **15** required to inhibit cell viability by 50 % after the incubation in the culture medium for 24 h. Along with the dark cytotoxicity, we determined the light cytotoxicity of these compounds under irradiation with a dose of 20 J/cm<sup>2</sup> ( $\lambda$  = 615-635 nm, power 20 mW/cm<sup>2</sup>) (Figure 6). The IC<sub>50</sub> values are summarized in Table 2. Despite the fact that A431 cells accumulate **12** in higher amounts than HeLa or CHO, their dark sensitivity to this compound seems to be lower. The differences in the cell lines sensitivity to the toxic agents are associated with their different metabolic activity and genes expression, and especially mutations in oncogenes that are specific for certain cancer cell lines. Also, while the accumulation of **15** is 5-10 folds lower in the investigated cell lines, its IC<sub>50dark</sub> values are 1.5-3 folds higher. Thus, this compound is several times more toxic for cells than **12**.

Conjugate **12** demonstrates photoinduced cytotoxicity in low-micromolar concentrations (2.0 – 3.0  $\mu\text{M}$ ), while its dark toxicity was 11-18 times lower. We observed slightly higher photoactivity of **12** against A431 (about two-fold increase in  $\text{IC}_{50\text{dark}}/\text{IC}_{50\text{light}}$ ). Compound **15**, lacking the molecular fragment responsible for the EGFR affinity was found to be less active, both in the dark and light conditions, with similar ratio between  $\text{IC}_{50\text{dark}}$  and  $\text{IC}_{50\text{light}}$ .

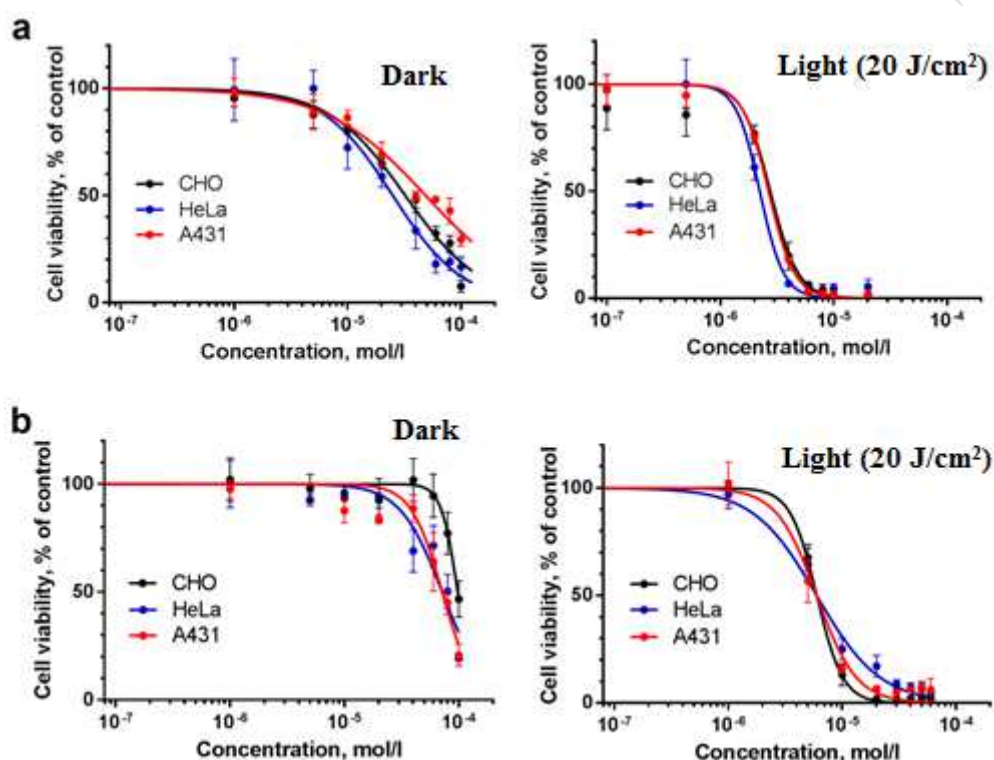


**Fig. 6.** Relative viability of CHO, HeLa and A431 cells after treatment with **12** (a) or **15** (b). Cells were incubated with the compound for 4 h, then the medium was exchanged with full fresh growth medium, and the cells were irradiated in dose 20  $\text{J}/\text{cm}^2$  ( $\lambda = 615\text{-}635$  nm, power 40  $\text{mW}/\text{cm}^2$ ) or stayed in dark. After the additional incubation for 24 h, cell viability was measured by MTT-assay and expressed as the percentage to untreated cells. Mean  $\pm$  SEM are presented; the experimental data are fitted using four parameters model for lognormal distribution.

**Table 2.** *In vitro* light and dark cytotoxic activity of **12** and **15**.

Cells	<b>12</b>		<b>15</b>	
	$\text{IC}_{50}$ , $\mu\text{M}$ [95% confidence]	$\text{IC}_{50\text{dark}}/\text{IC}_{50\text{light}}$	$\text{IC}_{50}$ , $\mu\text{M}$ [95% confidence]	$\text{IC}_{50\text{dark}}/\text{IC}_{50\text{light}}$
CHO				
HeLa				
A431				

	intervals]			intervals]		
	light	dark		light	dark	
<b>CHO</b>	2.7 [2.4;3.0]	32 [28;36]	12	6.1 [5.8;6.4]	>100	-
<b>HeLa</b>	2.2 [2.0;2.3]	25 [21;29]	11	6.5 [5.7;7.3]	72 [64;80]	11
<b>A431</b>	2.6 [2.5;2.7]	48 [43;55]	18	5.5 [4.9;6.2]	72 [63;81]	13

Ratio of  $IC_{50\text{dark}}/IC_{50\text{light}}$  for compound **12** in A431 cells is the highest of all the combinations tested. It correlates well with the increased uptake of **12** by A431 cells, expressing more EGFR than the other cell types (Fig. 5). We assume that the conjugate photoactivity is resulted from the same photochemical processes in all the cells, and its primary intracellular targets are also the same. In this case, the enhancement of A431 response to compound **12** can be a consequence of EGFR blockade.

Although  $IC_{50\text{dark}} / IC_{50\text{light}}$  is only 1.5-1.7 fold higher for this combination than for the others (excluding compound **15**/CHO cells, where the cells seem to be resistant to the dark toxicity of **15**), this demonstrate the efficiency of the agents for combined photodynamic treatment and the inhibition of growth factors receptors. We attribute the moderate increase to the comparably high non-specific binding of both compounds in the cells.

#### *Animal study*

After intravenous administration into the tumor-bearing Balb/c mice, compound **12** quickly disappears from the normal tissues, but shows relatively prolonged retention in the tumor (Figure 7). Its tumor-to-tissue ratio reaches 4.2 after 24 h. The behavior of compound **12** is similar to well-studied chlorin photosensitizer mTHPC, characterized by the tumor-to-skin ratio of ca. 4 [35], and a rather long period between the administration and the optimal PDT treatment time [36].

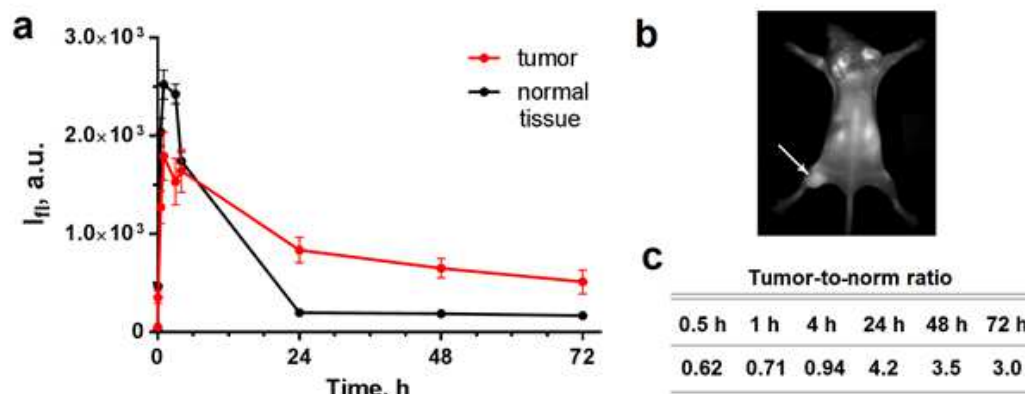


**Fig. 7.** Biodistribution of conjugate **12** *in vivo*.

(a) Dynamics of fluorescence intensity in tumor (red) and normal tissue (black) of the animals injected with conjugate **12**. Mean  $\pm$  SEM are presented ( $n=5$ ).  $\lambda_{ex}=615$  nm,  $\lambda_{em}=660-740$  nm. (b) Fluorescent image of a mouse, injected with **12** (24 h post-injection). Tumor is indicated by arrow. (c) Tumor-to-normal tissue fluorescence ratio at different time points, indicating selective accumulation of **12** in tumor.

These preliminary results demonstrate the ability of **12** to selectively accumulate in tumor cells and support the further development of this type of compounds as possible leads for tumor treatment.

### 3. Conclusions

In conclusion, we have synthesized a new water-soluble conjugate consisting of a chlorin-based photosensitizer and an EGFR/VEGFR ligand. The newly prepared hybrid molecules are of interest as a new class of theranostic agents. An increased accumulation of this compound in A431 cells with high EGFR expression was observed, in comparison with the uptake by the CHO and HeLa cells with low EGFR expression. The prepared conjugate exhibits dark and photoinduced cytotoxicity at low micromolar concentrations with pronounced  $IC_{50}^{dark}/IC_{50}^{light}$  ratio of 11-18. After intravenous administration into tumor-bearing mice, the conjugate preferentially accumulates in the tumor tissue as it was detected by fluorescence

measurements. The replacement of EGFR/VEGFR-binding part by another high affinity receptor ligand might be a simple way to change the selectivity of the conjugate action.

## 4. Experimental

### 4.1. Materials.

$^1\text{H}$  NMR and  $^{13}\text{C}$  NMR spectra were recorded on Agilent DD2 400 MHz spectrometer. Chemical shifts ( $\delta$ ) are reported in ppm for the solution of compound in  $\text{CDCl}_3$ ,  $\text{DMSO-d}_6$  or  $\text{CD}_3\text{OD}$ , with the residual peak of solvent as an internal reference,  $J$  values in Hertz. Mass spectra were recorded using the MALDI method on a time-of-flight Bruker Microflex LT mass-spectrometer. TLC analyses were carried out on Merck TLC Silica gel 60 F<sub>254</sub>. Column chromatography separation was performed using Macherey-Nagel Kieselgel 60 (70-230 mesh). Commercially available reagents (Aldrich, Alfa Aesar) were used without additional purification. Solvents were purified according to the standard procedures. Petroleum ether used was of bp 40-70 °C.

### 4.2. Preparation of compounds.

*Synthesis of 4-(amino-4'-bromo-2'-fluorophenyl)-6-methoxy-7-(3''-azidopropoxy)-quinazoline 2* [ $\text{C}_{18}\text{H}_{16}\text{BrFN}_6\text{O}_2$ ]. An argon-filled Schlenk flask was charged with quinazolinol **1** (0.250 g, 0.68 mmol), 1-bromo-3-chloropropane (0.125 g, 0.81 mmol) and  $\text{K}_2\text{CO}_3$  (0.283 g, 2.05 mmol). Anhydrous DMF (6 mL) was added, and the mixture was stirred for 24 h at 60 °C, cooled and concentrated under reduced pressure. The residue was dissolved in  $\text{CHCl}_3$  (100 mL), washed with  $\text{H}_2\text{O}$  ( $3 \times 50$  mL), dried ( $\text{Na}_2\text{SO}_4$ ), and concentrated in a Schlenk flask.  $\text{NaN}_3$  (0.165 g, 2.54 mmol), and anhydrous DMF (3 mL) were added, and the mixture was stirred for another 24 h at 50 °C. The solvent was removed under reduced pressure and the residue was dissolved in  $\text{CHCl}_3$  (100 mL), washed with  $\text{H}_2\text{O}$  ( $3 \times 50$  mL), dried ( $\text{Na}_2\text{SO}_4$ ), and concentrated. The product was purified by column chromatography (EtOAc/petroleum

ether 90:10) to obtain a white solid. Yield 0.215 g (70%); mp 142 °C. <sup>1</sup>H NMR: (400 MHz, DMSO-d<sub>6</sub>) δ 9.54(s, 1H, NH), 8.36 (s, 1H, CH), 7.80 (s, 1H, CH), 7.66 (d, *J* = 10 Hz, 1H, CH), 7.58-7.43 (m, 2H, 2CH), 7.21 (s, 1H, CH), 4.22 (t, *J* = 6.1 Hz, 2H, CH<sub>2</sub>), 3.95 (s, 3H, CH<sub>3</sub>O), 3.55 (t, *J* = 6.7 Hz, 2H, CH<sub>2</sub>), 2.12-2.00 (m, 2H, CH<sub>2</sub>). <sup>13</sup>C NMR: (101 MHz, DMSO-d<sub>6</sub>) δ 157.90, 156.88, 155.40, 153.44, 152.93, 149.01, 146.88, 129.55, 127.47, 126.44, 126.32, 119.43, 119.20, 117.99, 117.90, 108.72, 107.82, 102.01, 65.55, 56.15, 47.64, 27.91. MS (MALDI): *m/z* 447.1 [M+H]<sup>+</sup> (<sup>79</sup>Br), 449.1 [M+H]<sup>+</sup> (<sup>81</sup>Br).

*Synthesis of pheophorbide-a 4 [C<sub>35</sub>H<sub>36</sub>N<sub>4</sub>O<sub>5</sub>].* Conc. HCl (1 mL) was added dropwise to the solution of methylpheophorbide-*a* (0.300 g, 0.49 mmol) in acetone (15 mL). The mixture was stirred for 48 h at rt, diluted with CHCl<sub>3</sub> (200 mL), washed with H<sub>2</sub>O (3 × 100 mL), dried (Na<sub>2</sub>SO<sub>4</sub>), and concentrated. The product was purified by column chromatography (CHCl<sub>3</sub>/MeOH 95:5) to obtain a deep-green solid. Yield 0.272 g (93%). The physical and spectroscopic data obtained for the compound were in agreement with the published data [37].

*Synthesis of chlorin 6 [C<sub>38</sub>H<sub>39</sub>N<sub>5</sub>O<sub>4</sub>].* A Schlenk flask was filled with argon and charged with EDC·HCl (0.138 g, 0.72 mmol) and pheophorbide-*a* (**4**, 0.213 g, 0.36 mmol). Anhydrous CHCl<sub>3</sub> (4 mL) was added, and the mixture was stirred for 30 min at 0 °C. Another flask was charged with propargyl amine (**5**, 0.04 g, 0.73 mmol), DMAP (0.022 g, 0.18 mmol) and anhydrous CHCl<sub>3</sub> (4 mL). The mixture from the second flask was transferred by a syringe into the first flask. The reaction mixture was stirred at 0 °C for 1 h, at rt for 18 h, and concentrated under reduced pressure. The residue was dissolved in CHCl<sub>3</sub> (100 mL), washed with H<sub>2</sub>O (3 × 100 mL), dried (Na<sub>2</sub>SO<sub>4</sub>), and concentrated. The product was purified by column chromatography (CHCl<sub>3</sub>/MeOH 98:2) to obtain a deep-green solid. Yield 0.188 g (81%); mp 139 °C. <sup>1</sup>H NMR: (400 MHz, CDCl<sub>3</sub>) δ 9.49 (br.s, 2H), 8.63 (s, 1H), 7.98 (dd, *J* = 17.5, 11.5 Hz, 1H), 6.30 (d, *J* = 18.2 Hz, 1H), 6.27 (s, 1H), 6.20 (d, *J* = 19.9 Hz), 5.36 (br.s, 1H), 4.53 (br.s, 1H), 4.27 (br.s, 1H), 3.87 (s, 3H), 3.78-3.55 (m, 7H), 3.41 (s, 3H), 3.25 (s, 3H), 2.70 (br.s, 1H), 2.46 (br.s, 1H), 2.33-2.15 (m, 2H), 1.94 (s, 1H), 1.83 (d, *J* = 6.6 Hz, 3H), 1.68 (t, *J*

ACCEPTED MANUSCRIPT  
= 7.6 Hz), -1.66 (br.s, 2H).  $^{13}\text{C}$  NMR: (101 MHz,  $\text{CDCl}_3$ )  $\delta$  189.36, 172.27, 171.76, 169.56, 137.93, 128.86, 104.64, 104.26, 97.59, 79.16, 64.77, 52.97, 51.52, 50.25, 29.69, 28.83, 23.31, 19.55, 17.19, 12.16, 11.26. MS (MALDI):  $m/z$  630.1  $[\text{M}]^+$ .

*Synthesis of chlorin 8* [ $\text{C}_{42}\text{H}_{49}\text{N}_7\text{O}_4\text{Zn}$ ]. Amine **7** (0.640 g, 7.34 mmol) was added to a solution of chlorin **6** (0.180 g, 0.29 mmol) in  $\text{CHCl}_3$  (7 mL), and the mixture was stirred at rt, until **6** was completely consumed (TLC). Solution of  $\text{Zn}(\text{OAc})_2$  (0.360 g, 1.97 mmol) in MeOH (3 mL) was added, the mixture was stirred for 2 h, then diluted with  $\text{CHCl}_3$  (100 mL) and washed with  $\text{H}_2\text{O}$  ( $3 \times 50$  mL). The organic phase was dried ( $\text{Na}_2\text{SO}_4$ ) and concentrated under reduced pressure. The product was purified by column chromatography ( $\text{CHCl}_3/\text{MeOH}$  95:5 to 85:15) to obtain a deep-green solid. Yield 0.205 g (92%); mp 145 °C.  $^1\text{H}$  NMR: (400 MHz,  $\text{DMSO-d}_6$ )  $\delta$  9.51 (s, 2H), 8.96 (br.s, 1H), 8.66 (s, 1H), 8.34 (t,  $J = 5.4$  Hz, 1H), 8.22 (dd,  $J = 17.8, 11.6$  Hz, 1H), 6.22 (d,  $J = 17.9$  Hz, 1H), 6.00 (d,  $J = 11.6$  Hz, 1H), 5.41 (d,  $J = 19.1$  Hz, 1H), 5.07 (d,  $J = 18.9$  Hz, 1H), 4.42 (q,  $J = 7.0$  Hz, 1H), 4.20 (d,  $J = 9.9$  Hz, 1H), 3.91- 3.75 (m, 6H), 3.69 (br.s, 4H), 3.37 (s, 3H), 3.35 (s, 3H), 3.26-3.16 (m, 3H), 3.05 (t,  $J = 2.3$  Hz, 1H), 2.73 (br.s, 6H), 2.47-2.38 (m, 1H), 2.07 (d,  $J = 8.8$  Hz, 2H), 1.67 (t,  $J = 7.5$  Hz, 3H), 1.61 (d,  $J = 7.0$  Hz).  $^{13}\text{C}$  NMR: (101 MHz,  $\text{DMSO-d}_6$ )  $\delta$  173.24, 171.72, 170.35, 165.14, 162.77, 151.66, 147.96, 146.14, 144.07, 143.10, 141.20, 140.74, 138.58, 137.23, 133.04, 132.29, 130.66, 119.20, 101.79, 101.75, 99.87, 93.16, 81.19, 72.81, 52.24, 51.65, 46.26, 43.88, 37.46, 32.02, 29.99, 27.78, 22.80, 18.87, 17.89, 12.30, 11.76, 10.93. MS (MALDI):  $m/z$  779.0  $[\text{M}]^+$ .

*Synthesis of conjugate 9* [ $\text{C}_{60}\text{H}_{65}\text{BrFN}_{13}\text{O}_6\text{Zn}$ ]. Chlorin **8** (0.060 g, 0.08 mmol) and compound **2** (0.045, 0.09 mmol) were placed in a flask with mixture of *t*-BuOH/ $\text{CHCl}_3/\text{H}_2\text{O}$  (2:1:2) (9 mL). In another flask,  $\text{CuSO}_4 \cdot 5\text{H}_2\text{O}$  (0.005 g, 0.02 mmol), TBTA (0.008 g, 0.01 mmol) and sodium ascorbate (0.006 g, 0.03 mmol) were dissolved in 6 mL  $\text{H}_2\text{O}$ , and this solution was immediately added into the first flask. The mixture was stirred for 1.5 h at 50 °C, cooled, diluted with  $\text{CHCl}_3$  (100 mL), washed with  $\text{H}_2\text{O}$  ( $3 \times 50$  mL), dried ( $\text{Na}_2\text{SO}_4$ ), and

concentrated. The product was purified by column chromatography (CHCl<sub>3</sub>/MeOH 95:5 to 80:20) to obtain a deep-green solid. Yield 0.068 g (72%); mp 175 °C. <sup>1</sup>H NMR: (400 MHz, DMSO-d<sub>6</sub>) δ 10.81 (s, 1H), 9.50 (s, 1H), 9.47 (s, 1H), 9.16 (br.s, 1H), 8.57 (s, 1H), 8.51 (br.s, 1H), 8.20 (dd, *J* = 17.8, 11.7 Hz, 1H), 8.04 (s, 1H), 7.80 (br.s, 1H), 7.61 (d, *J* = 9.9 Hz, 7.55-7.26 (m, 3H), 6.20 (d, *J* = 18.2 Hz, 1H), 5.99 (d, *J* = 11.8 Hz, 1H), 5.23 (br.s, 2H), 4.53 (br.s, 2H), 4.44-4.33 (m, 2H), 4.26 (d, *J* = 5.1 Hz, 1H), 4.18-4.09 (m, 1H), 4.07-4.01 (m, 1H), 4.00-3.88 (m, 3H), 3.86 (s, 3H), 3.83-3.73 (m, 2H), 3.67 (s, 3H), 3.56-3.48 (m, 2H), 3.25-3.16 (m, 4H), 2.98 (s, 6H), 2.44-2.26 (m, 4H), 2.07 (d, *J* = 8.2 Hz, 2H), 1.65 (t, *J* = 7.4 Hz, 3H), 1.45 (d, *J* = 6.0 Hz, 3H). <sup>13</sup>C NMR: (101 MHz, DMSO-d<sub>6</sub>) δ 173.52, 171.94, 170.28, 165.09, 162.46, 157.82, 156.65, 155.32, 153.18, 152.15, 151.63, 148.70, 148.03, 146.21, 145.13, 144.15, 143.13, 141.18, 140.84, 139.00, 137.20, 133.37, 133.03, 132.39, 130.59, 129.59, 127.46, 125.97, 125.85, 122.73, 119.39, 119.22, 119.16, 117.89, 117.81, 113.79, 108.03, 102.31, 101.99, 101.96, 99.95, 93.19, 65.21, 57.70, 56.14, 52.80, 52.17, 51.62, 46.27, 46.10, 43.90, 37.19, 34.06, 32.08, 29.56, 22.71, 18.86, 17.85, 12.28, 11.82, 10.92. MS (MALDI): *m/z* 1226.6 [M+H]<sup>+</sup>.

*Synthesis of conjugate 11 [C<sub>66</sub>H<sub>79</sub>BrFN<sub>15</sub>O<sub>6</sub>Zn].* Bis(dimethylamino)methane (**10**, 0.524 g, 5.14 mmol) was added to a solution of conjugate **9** (0.070 g, 0.06 mmol) in AcOH/THF (1:1, 8 mL), and the mixture was stirred for 1 h at rt. It was diluted with CHCl<sub>3</sub> (100 mL), washed with 2% NaOH (3 × 100 mL) and H<sub>2</sub>O (1 × 100 mL), dried (Na<sub>2</sub>SO<sub>4</sub>), and concentrated. The product was purified by column chromatography (CHCl<sub>3</sub>/MeOH-Et<sub>3</sub>N 97:2:1 to 95:5:1) to obtain a deep-green solid. Yield 0.048 g (63%); mp 174 °C. <sup>1</sup>H NMR: (400 MHz, DMSO-d<sub>6</sub>) δ 9.61 (s, 1H), 9.46 (s, 1H), 9.43 (br.s, 1H), 8.73 (s, 1H), 8.57 (br.s, 1H), 8.51 (s, 1H), 8.10 (s, 1H), 7.61-7.50 (m, 3H), 7.43-7.24 (m, 2H), 7.23-7.10 (m, 1H), 5.26 (br.s, 2H), 4.59-4.51 (m, 2H), 4.51-4.41 (m, 2H), 4.34 (d, *J* = 6.8 Hz, 1H), 4.27-4.19 (m, 1H), 4.16-4.11 (m, 2H), 4.05-3.89 (m, 3H), 3.82 (br.s, 8H), 3.64 (br.s, 5H), 3.61-3.49 (m, 3H), 3.26-3.13 (m, 4H), 2.71-2.66 (m, 3H), 2.35 (br.s, 10H), 2.22-2.13 (m, 10H), 2.11-1.99 (m, 3H), 1.66 (t, *J* = 7.4 Hz, 3H),

1.39 (d,  $J = 6.8$  Hz, 3H).  $^{13}\text{C}$  NMR: (101 MHz,  $\text{CD}_3\text{OD}$ )  $\delta$  179.04, 176.43, 175.30, 174.12, 166.97, 163.45, 159.21, 158.25, 156.70, 155.14, 153.61, 152.90, 150.88, 149.13, 148.65, 146.57, 145.76, 145.58, 145.30, 142.98, 142.78, 140.96, 139.51, 136.20, 134.63, 133.32, 130.09, 128.29, 126.38, 124.64, 120.41, 120.17, 119.65, 109.34, 103.96, 103.01, 102.16, 102.02, 94.19, 66.10, 58.99, 57.43, 56.70, 53.87, 52.69, 48.16, 47.67, 45.35, 44.24, 39.18, 38.71, 35.35, 33.49, 30.68, 23.43, 23.32, 20.29, 18.15, 14.20, 13.20, 12.13, 11.37, 11.21. MS (MALDI):  $m/z$  1343.9  $[\text{M}+\text{H}]^+$ .

*Synthesis of conjugate 12* [ $(\text{C}_{69}\text{H}_{88}\text{BrFN}_{15}\text{O}_6\text{Zn})\text{I}_3$ ].  $\text{CH}_3\text{I}$  (0.228 g, 1.60 mmol) was added to a solution of conjugate **11** (0.025 g, 0.02 mmol) in THF (5 mL), and the mixture was stirred at rt until a precipitate formed. It was collected on a filter, washed with a small amount of THF and dried under reduced pressure to obtain a deep-green solid. Yield 0.032 g (quantitative); mp 168 °C.  $^1\text{H}$  NMR: (400 MHz,  $\text{DMSO-d}_6$ )  $\delta$  9.59 (d,  $J = 10.6$  Hz, 1H), 9.50 (br.s, 2H), 9.19 (s, 1H), 8.57 (br.s, 2H), 8.07 (s, 1H), 7.95 (s, 1H), 7.68-7.51 (m, 2H), 7.45-7.32 (m, 2H), 7.23-7.05 (m, 1H), 5.23 (br.s, 2H), 4.55 (br.s, 2H), 4.48-4.34 (m, 2H), 4.32-4.19 (m, 2H), 4.12 (br.s, 2H), 4.04-3.89 (m, 3H), 3.86-3.78 (m, 11H), 3.69 (s, 5H), 3.10 (br.s, 12H), 2.89 (s, 9H), 2.73 (s, 9H), 2.45-2.29 (m, 3H), 2.18 (d,  $J = 6.5$  Hz, 3H), 2.13-1.94 (m, 3H), 1.65 (t,  $J = 6.8$  Hz, 3H), 1.43 (d,  $J = 5.8$  Hz, 3H).  $^{13}\text{C}$  NMR: (101 MHz,  $\text{DMSO-d}_6$ )  $\delta$  173.42, 171.93, 169.85, 162.71, 157.86, 156.92, 156.70, 155.36, 153.21, 148.76, 147.87, 146.10, 145.09, 143.33, 141.15, 140.98, 133.18, 132.82, 129.59, 127.50, 122.78, 119.41, 119.19, 117.85, 102.06, 99.55, 93.27, 65.24, 63.65, 56.16, 54.91, 52.78, 52.38, 51.77, 46.28, 37.30, 34.04, 32.10, 31.28, 30.39, 29.51, 29.00, 27.88, 22.70, 21.05, 18.85, 17.88, 13.96, 11.91, 11.06.

*Synthesis of chlorin 13* [ $\text{C}_{40}\text{H}_{48}\text{N}_6\text{O}_5\text{Zn}$ ]. Compound **7** (0.807 g, 9.17 mmol) was added to a solution of methylpheophorbide-*a* (**3**, 0.200 g, 0.33 mmol) in  $\text{CHCl}_3$  (8 mL), and the mixture was stirred at rt until **3** was completely consumed (TLC). Solution of  $\text{Zn}(\text{OAc})_2$  (0.300 g, 1.64 mmol) in MeOH (3 mL) was added, the mixture was stirred for 2 h, diluted with  $\text{CHCl}_3$  (100 mL) and washed with  $\text{H}_2\text{O}$  ( $3 \times 50$  mL). The organic phase was dried ( $\text{Na}_2\text{SO}_4$ ) and

concentrated under reduced pressure. The product was purified by column chromatography (CHCl<sub>3</sub>/MeOH 98:2 to 90:10) to obtain a deep-green solid. Yield: 0.180 g (72%); mp 138 °C. <sup>1</sup>H NMR: (400 MHz, DMSO-d<sub>6</sub>) δ 9.53 (s, 1H), 9.51 (s, 1H), 8.71 (t, *J* = 5.3 Hz, 1H), 8.66 (s, 1H), 8.23 (dd, *J* = 17.8, 11.6 Hz, 1H), 6.22 (d, *J* = 17.9 Hz, 1H), 6.01 (d, *J* = 11.6 Hz, 1H), 5.43 (d, *J* = 19.1 Hz, 1H), 5.13 (d, *J* = 19.1 Hz, 1H), 4.43 (q, *J* = 6.9 Hz, 1H), 4.28 (d, *J* = 9.2 Hz, 1H), 3.82 (q, *J* = 7.5 Hz, 2H), 3.67 (s, 3H), 3.54 (s, 3H), 3.37 (s, 3H), 3.27-3.16 (m, 1H), 2.67 (t, *J* = 6.9 Hz, 2H), 2.61-2.54 (m, 1H), 2.33 (s, 6H), 2.12 (d, *J* = 10.1 Hz, 2H), 1.68 (t, *J* = 7.5 Hz, 3H), 1.60 (d, *J* = 7.0 Hz, 3H). <sup>13</sup>C NMR: (101 MHz, DMSO-d<sub>6</sub>) δ 173.34, 173.28, 169.91, 164.97, 162.11, 151.62, 148.15, 146.06, 144.00, 143.15, 141.40, 140.73, 138.56, 137.23, 134.06, 133.05, 132.24, 130.69, 119.20, 101.99, 101.75, 99.95, 93.04, 58.11, 51.98, 51.59, 51.26, 46.11, 45.36, 37.68, 37.35, 30.01, 29.19, 22.84, 18.90, 17.92, 12.31, 11.68, 10.95. MS (MALDI): *m/z* 755.9 [M]<sup>+</sup>.

*Synthesis of chlorin 14 [C<sub>46</sub>H<sub>62</sub>N<sub>8</sub>O<sub>5</sub>Zn].* Bis(dimethylamino)methane (**10**, 0.749 g, 7.34 mmol) was added to a solution of chlorin **13** (0.150 g, 0.20 mmol) in mixture of AcOH/THF (1:1) (10 mL), and the mixture was stirred for 1 h at rt. It was diluted with CHCl<sub>3</sub> (100 mL), washed with 2% NaOH (3 × 100 mL) and H<sub>2</sub>O (100 mL), dried (Na<sub>2</sub>SO<sub>4</sub>), and concentrated. The product was purified by column chromatography (CHCl<sub>3</sub>/MeOH/Et<sub>3</sub>N from 98:1:1 to 96:3:1) to obtain a deep-green solid. Yield 0.132 g (76%); mp 155 °C. <sup>1</sup>H NMR: (400 MHz, DMSO-d<sub>6</sub>) δ 9.63 (s, 1H), 9.52 (s, 1H), 8.71 (br.s, 1H), 8.62 (s, 1H), 7.21-7.12 (m, 1H), 5.44 (d, *J* = 18.6 Hz, 1H), 5.13 (d, *J* = 19.1 Hz, 1H), 4.43 (d, *J* = 7.0 Hz, 1H), 4.28 (d, *J* = 9.3 Hz, 1H), 3.82 (d, *J* = 7.3 Hz, 2H), 3.67 (br.s, 5H), 3.55 (br.s, 5H), 2.76-2.70 (m, 1H), 2.66 (t, *J* = 6.9 Hz, 2H), 2.62-2.53 (m, 1H), 2.32 (br.s, 9H), 2.16 (br.s, 11H), 1.68 (t, *J* = 7.3 Hz, 3H), 1.59 (br.s, 3H). <sup>13</sup>C NMR: (101 MHz, DMSO-d<sub>6</sub>) δ 173.33, 173.27, 170.02, 164.97, 162.09, 151.14, 148.12, 145.70, 143.17, 142.88, 142.82, 141.37, 140.71, 138.59, 138.49, 134.10, 133.55, 133.39, 132.81, 102.01, 101.76, 100.50, 92.97, 69.55, 58.14, 55.50, 51.98, 51.59,

51.27, 46.11, 45.40, 45.17, 37.73, 37.34, 30.09, 29.16, 22.82, 18.90, 17.91, 11.67, 11.29, 10.89. MS (MALDI):  $m/z$  872.9  $[M]^+$ .

*Synthesis of chlorin 15 [(C<sub>49</sub>H<sub>71</sub>N<sub>8</sub>O<sub>5</sub>Zn)I<sub>3</sub>].* CH<sub>3</sub>I (0.228 g, 1.60 mmol) was added to a solution of chlorin **14** (0.03 g, 0.03 mmol) in THF (5 mL), and the mixture was stirred at rt until a precipitate formed. It was collected on a filter, washed with a small amount of THF and dried under reduced pressure to give a deep-green solid. Yield 0.032 g (quantitative); mp 151 °C. <sup>1</sup>H NMR: (400 MHz, DMSO-d<sub>6</sub>) δ 9.62 (d,  $J$  = 15.2 Hz, 1H), 9.56 (s, 1H), 9.19 (br.s, 1H), 8.66 (s, 1H), 7.23-7.10 (m, 1H), 5.37 (d,  $J$  = 19.0 Hz, 1H), 5.13 (d,  $J$  = 19.1 Hz, 1H), 4.45 (d,  $J$  = 6.9 Hz, 1H), 4.32 (d,  $J$  = 8.2 Hz, 1H), 4.03-3.77 (m, 6H), 3.72 (s, 3H), 3.54 (s, 3H), 3.16 (br.s, 9H), 2.86 (br.s, 1H), 2.65-2.55 (m, 1H), 2.22 (d,  $J$  = 14.7 Hz, 2H), 2.17-2.08 (m, 2H), 1.71-1.65 (m, 3H), 1.60 (br.s, 3H). <sup>13</sup>C NMR: (101 MHz, DMSO-d<sub>6</sub>) δ 173.30, 173.23, 170.71, 165.32, 162.21, 151.07, 147.77, 146.11, 143.33, 142.61, 142.47, 141.14, 141.02, 138.87, 137.15, 134.05, 133.24, 132.82, 102.08, 101.89, 97.17, 93.18, 75.19, 68.76, 68.28, 65.71, 63.64, 62.72, 52.80, 52.42, 51.84, 51.30, 37.53, 34.00, 29.94, 29.14, 22.76, 18.86, 17.92, 11.88, 11.45, 11.07.

### 4.3. Photophysical measurements

Photophysical properties of **12** and **15** were measured in deionized water at 5 μM solutions.

Absorption and fluorescence spectra were registered using a Synergy MX spectrophotometer-spectrofluorometer (BioTek, USA). Fluorescence was excited at 410 nm.

The molar extinction coefficient  $\varepsilon$  was determined using the following equation:

$$\varepsilon = D/cl,$$

where  $D$  – optical density;  $l$  – path length;  $c$  – concentration.

The fluorescence quantum yield  $\varphi_f$  was calculated using the equation:

$$\varphi_f = \frac{\varphi_2 F_1 D_2}{F_2 D_1},$$

where  $F_i$  and  $D_i$  – integral fluorescence intensity and optical density of **12** (or **15**), respectively;

$\phi_2$  – quantum yield of Rhodamine B (Sigma, USA) in water (0.31);  $F_2$  and  $D_2$  – integral fluorescence intensity and optical density of rhodamine B, respectively.

The fluorescence was excited at 410 nm, the optical density was measured at the same wavelength. The fluorescence signal was detected at 550–850 nm.

#### 4.4 Cell lines and culturing conditions

Cell lines of human epidermoid carcinoma A431, human cervical carcinoma HeLa, chinese hamster ovary CHO were obtained from the Russian cell culture collection of vertebrates. The cells were cultured in Eagle MEM medium (PanEco, Russia) with 10% (v/v) fetal calf serum (HyClone, USA) and 2 mM L-glutamine in 5% CO<sub>2</sub> at 37 °C. At each passaging stage the cells were treated with Versene solution (PanEco, Russia).

Cells of mouse colon adenocarcinoma CT-26 (ATCCnumber CRL-2638) were cultured in RPMI medium (HyClone, USA) with the same supplements and treated with 0.25% trypsin-EDTA solution (PanEco, Russia) at passaging stages.

#### 4.5. EGFR analysis

Cells ( $0.3 \times 10^6$ ) were detached from culturing flask and resuspended in 500  $\mu$ l 3% (w/v) solution of bovine serum albumin (BSA) in phosphate-buffered saline (PBS). Anti-EGFR antibodies conjugated with phycoerythrin (Abcam, UK) were added (0.1  $\mu$ g/m, 3  $\mu$ l), the cells were incubated for 30 min under rotation at 15 rpm, and then washed twice with 1% BSA in PBS.

Fluorescence of the stained cells was immediately analyzed using FACSCalibur flow cytometer (BD Biosciences, USA) using 488 nm laser and registration of phycoerythrin (PE) emission at 585/42 nm. 30 000 cells were analyzed for every cell line.

To assess nonspecific antibodies adherence on cell surface, the cells were stained by antibodies of the same isotype conjugated with phycoerythrin (Abcam, UK) having no specific target on cell surfaces and undergo the same flow cytometry procedure (isotypic control).

Ratio of geometric mean fluorescence intensities in EGFR-labeled and isotype control cells was calculated to express the relative level of EGFR expression.

#### 4.6. Study of cellular uptake

Cells were seeded in glass bottom 96-well plates (Falcon, Germany) at the density of  $4 \times 10^3$  cells per well and allowed to attach overnight. The medium was then exchanged with fresh serum-free growth medium containing 5  $\mu$ M of tested compound. Cells were incubated for 4 hours, washed thrice with PBS, fixed with 4% formaldehyde for 30 min and washed again.

Cells were imaged using laser scanning confocal microscope Axio Observer Z1 LSM 710 NLO/Duo (Carl Zeiss, Germany) equipped with C-Apochromat 63 $\times$ water immersion objective lens with numerical aperture 1.2. Fluorescence was excited at 405 nm and registered in the range of 600-740 nm.

The fluorescence intensity of the cytoplasmic region of the cells was measured using ZEN 2012 program; at least 10 cells in two-three fields of view were analyzed.

#### 4.7. Cytotoxicity study

The effect of tested compounds on cell viability was estimated using the microculture tetrazoline test (MTT) [38].

Cells were seeded in 96-well plates at the density of  $4 \times 10^3$  cells per well and allowed to attach overnight. The medium was then exchanged with fresh serum-free growth medium containing tested compound in different concentration. After 4 h of incubation, the medium was exchanged with full fresh growth medium.

To estimate the photoinduced toxicity of the tested compound, the cells were exposed to light irradiation (615–635 nm, 20 mW/cm<sup>2</sup>, 20 J/cm<sup>2</sup>) using LED light source providing a homogeneous light distribution in 96-well plates [39]. Irradiated cells were then incubated for 24 h before cell viability was measured. To this aim, the cells were incubated with serum-free medium containing 0.5 mg/mL MTT-reagent (3-(4,5-dimethyl-2-thiazolyl)-2,5-diphenyl-2H-tetrazole bromide, Alfa Aesar, USA) for 4 hours. The formazan formed from the reduction of

MTT by cells' dehydrogenases was dissolved in DMSO, and the absorbance was measured at 570 nm with a Synergy MX plate reader (BioTeck, USA).

A similar procedure was used for the estimation of the dark toxicity. The cells, grown overnight, were incubated in the medium with the compound being tested, washed with full fresh growth medium, then incubated for 24 h and undergo MTT assay.

Cell viability was expressed as the ratio of the optical density of treated and untreated cells (in percentage). Three independent experiments (all in triplicate) were performed. Experimental data were fitted using four parameters model for lognormal distribution to obtain dose-effect relationship and calculate inhibition concentration  $IC_{50}$ :

$$Y = Y_{\min} + \frac{Y_{\max} - Y_{\min}}{1 + 10^{(\lg(IC_{50}) - X) \cdot SF}},$$

where  $Y_{\max}$  and  $Y_{\min}$  – maximal and minimal Y values, respectively; SF –slope factor.

Data analysis was performed using the GraphPad Prism 6 software.

#### 4.8. Animal study

Balb/c female mice (age 8 weeks; 17 g, n=5) were inoculated subcutaneously in the left leg with  $10^6$  CT-26 cells in 0.2 mL PBS. Nine days after the inoculation, when tumors reached  $\sim 100 \text{ mm}^3$ , the mice were injected with conjugate **12** solved in PBS, in dose 25  $\mu\text{g}/\text{kg}$  intravenously into the tail vein.

Whole-body *in vivo* fluorescence imaging was performed using a fluorescence imaging system (Institute of Applied Physics RAS, Russia). Fluorescence was excited using narrow-band LED with central wavelength 615 nm and collected with cooled CCD-camera (ORCA II BT-512G, Hamamatsu Photonics K.K., Japan) in the range 660-740 nm. Images were obtained before and at different time points post-injection.

All experimental procedures were approved by the local Committee on Bioethics (protocol No. 7 of 06 July 2017).

The mean signal was calculated using ImageJ software in two regions of interest (ROI): tumor area and a region of the same area and position on the other leg ('normal tissue').

**ACKNOWLEDGEMENTS**

We thank the Russian Foundation of Basic Research (grant number 16-03-00464). O.I. Koifman thank the Ministry of Education and Science of the Russian Federation (government assignment number 4 1929.2017-4.6)

**Supplementary data**

The following is the supplementary data related to this article:

$^1\text{H}$ ,  $^{13}\text{C}$  NMR, IR and MS spectra.

**Corresponding Authors**

\*(I.V.B.) Tel/Fax: +7 831-462-32-13. E-mail: [irin-b@mail.ru](mailto:irin-b@mail.ru)

\*(A.Yu.F.) Fax: +7 831-462-30-85. E-mail: [afnn@rambler.ru](mailto:afnn@rambler.ru)

**Notes**

The authors declare no competing financial interest.

**REFERENCES**

- [1] (a) D. Van Straten, V. Mashayekhi, H.S. de Bruijn, S. Oliveira, D.J. Robinson, Oncologic photodynamic therapy: basic principles, current clinical status and future direction, *Cancers*, 9 (2017) 19; (b) E.J. Dennis, G.J. Dolmans, D. Fukumura, R.K. Jain, Photodynamic therapy for cancer, *Nat. Rev. Cancer* 3 (2003) 380–387; (c) P. Agostinis, K. Berg, K.A. Cengel, T.H. Foster, A.W. Girotti, S.O. Gollnick, S.M. Hahn, M.R. Hamblin, A. Juzeniene, D. Kessel, M. Korbelik, J. Moan, P. Mroz, D. Nowis, J. Piette, B.C. Wilson, J. Golab, Photodynamic therapy of cancer: an update, *CA Cancer J. Clin.* 61 (2011) 250–281; (d) C.A. Robertson, D. Hawkins Evans, H. Abrahamse, Photodynamic therapy (PDT): a short review on cellular mechanisms and cancer research applications for PDT, *J. Photochem. Photobiol. B* 96 (2009) 1–8.
- [2] (a) M.T. Wan, J.Y. Lin, Current evidence and applications of photodynamic therapy in dermatology, *Clin. Cosmet. Investig. Dermatol.* 7 (2014) 145–163; (b) P. Babilas, S. Schreml,

M. Landthaler, R.-M. Szeimies, Photodynamic therapy in dermatology: state-of-the-art, *Photodermatol. Photoimmunol. Photomed.* 26 (2010) 118–132; (c) S. Choudhary, K. Nouri, M.L. Elsaie, Photodynamic therapy in dermatology: a review, *Lasers Med. Sci.* 24 (2009) 971–980; (d) R. Darlenski, J.W. Fluhr, Photodynamic therapy in dermatology: past, present, and future, *J. Biomed. Opt* 18 (2012) 061208.

[3] (a) J. Marotti, A.C.C. Aranha, C.D.P. Eduardo, M.S. Ribeiro, Photodynamic therapy can be effective as a treatment for herpes simplex labialis, *Photomed. Laser Surg.* 27 (2009) 357–363; (b) M.E. Lima, Y.-I. Leeb, Y. Zhanga, J. Jang Hann Chu, Photodynamic inactivation of viruses using upconversion nanoparticles, *Biomaterials* 33 (2012) 1912–1920.

[4] (a) R.F. Donnelly, P.A. McCarron, M.M. Tunney, Antifungal photodynamic therapy, *Microbiol. Res.* 163 (2008) 1-12; (b) J.P. Lyon, C. de M.P. e S. Azevedo, L.M. Moreira, C. José de Lima, M.A. de Resende, Photodynamic Antifungal Therapy Against Chromoblastomycosis, *Mycopathologia* 172 (2011) 293–297.

[5] (a) A.A. Takasaki, A. Aoki, K. Mizutani, F. Schwarz, A. Sculean, C.-Y. Wang, G. Koshy, G. Romanos, I. Ishikawa, Y. Izumi, Application of antimicrobial photodynamic therapy in periodontal and peri-implant diseases, *Periodontol.* 2000 51 (2009) 109–140; (b) A. Tavares, S.R.S. Dias, C.M.B. Carvalho, M.A. Faustino, M.G.P.M.S. Neves, J.P.C. Tomé, A.C. Tomé, J.A.S. Cavaleiro, Â. Cunha, N.C.M. Gomes, E. Alves, A. Almeida, Mechanisms of photodynamic inactivation of a Gram-negative recombinant bioluminescent bacterium by cationic porphyrins, *Mar. Drugs* 8 (2010) 91–105.

[6] A.T. Dharmaraja, Role of reactive oxygen species (ROS) in therapeutics and drug resistance in cancer and bacteria, *J. Med. Chem.* 60 (2017) 3221–3240.

[7] P. Mroz, A. Yaroslavsky, G.B. Kharkwal, M.R. Hamblin, Cell death pathways in photodynamic therapy of cancer, *Cancers* 3 (2011) 2516–2539.

[8] (a) R.J.Y. Ho, J. Chien, Trends in translational medicine and drug targeting and delivery: new insights on an old concept—targeted drug delivery with antibody–drug conjugates for

cancers, *J. J. Pharm. Sci.* 103 (2014) 71–77; (b) L. Dai, J. Liu, Z. Luo, M. Li, K. Cai, Tumor therapy: targeted drug delivery systems, *J. Mater. Chem. B* 4 (2016) 6758–6772; (c) T. Luhmann, L. Meinel, Nanotransporters for drug delivery, *Curr. Opin. Biotechnol* 39 (2016) 35–40; (d) H.-J. Hsu, J. Bugno, S. Lee, S. Hong. Dendrimer-based nanocarriers: a versatile platform for drug delivery, *WIREs Nanomed. Nanobiotechnol* 9 (2016) 1409; (e) S.Z. Vahed, R. Salehi, S. Davaran, S. Sharifi, Liposome-based drug co-delivery systems in cancer cells, *Mater. Sci. Eng. C* 71 (2017) 1327–1341; (f) M.A. Grin, A.F. Mironov, A.A. Shtil, Anti-cancer agents in medicinal chemistry (Formerly Current Medicinal Chemistry - Anti-Cancer Agents) 8 (2008) 683–697.

[9] (a) P.R. Hamann, L.M. Hinman, I. Hollander, C.F. Beyer, D. Lindh, R. Holcomb, W. Hallett, H.-R. Tsou, J. Upešlacis, D. Shochat, A. Mountain, D.A. Flowers, I. Bernstein, Gemtuzumab Ozogamicin, A potent and selective anti-CD33 antibody–calicheamicin conjugate for treatment of acute myeloid leukemia, *Bioconjugate Chem.* 13 (2002) 47–58; (b) A. Gabizon, H. Shmeeda, Y. Barenholz, Pharmacokinetics of pegylated liposomal doxorubicin, *Clin. Pharmacokinet* 42 (2003) 419–436; (c) J.D. Bagnato, A.L. Eilers, R.A. Horton, C.B. Grissom, Synthesis and characterization of a cobalamin–colchicine conjugate as a novel tumor-targeted cytotoxin, *J. Org. Chem.* 69 (2004) 8987–8996. (d) A. Homma, H. Sato, A. Okamachi, T. Emura, T. Ishizawa, T. Kato, T. Matsuura, S. Sato, T. Tamura, Y. Higuchi, T. Watanabe, H. Kitamura, K. Asanuma, T. Yamazaki, M. Ikemi, H. Kitagawa, T. Morikawa, H. Ikeya, K. Maeda, K. Takahashi, K. Nohmi, N. Izutani, M. Kanda, R. Suzuki, Novel hyaluronic acid–methotrexate conjugates for osteoarthritis treatment, *Biorg. Med. Chem.* 17 (2009) 4647–4656; (e) B. Moulari, A. Béduneau, Y. Pellequer, A. Lamprecht, Lectin-decorated nanoparticles enhance binding to the inflamed tissue in experimental colitis, *J. Control. Release* 188 (2014) 9–17; (f) P. Ringhieri, C. Diaferia, S. Galdiero, R. Palumbo, G. Morelli, A. Accardo, Liposomal doxorubicin doubly functionalized with CCK8 and R8 peptide sequences for selective intracellular drug delivery, *J. Pept. Sci.* 21 (2015) 415–425;

- (g) L.Q. Chen, W. Huang, Z.G. Gao, W.S. Fang, M. Jin, Lx2-32c-loaded polymeric micelles with small size for intravenous drug delivery and their inhibitory effect on tumor growth and metastasis in clinically associated 4T1 murine breast cancer, *J. Int. J. Nanomedicine* 11 (2016) 5457–5472; (h) H.J. Lee, H.H. Park, Y. Sohn, J. Ryu, J.H. Park, W.J. Rhee, T.H. Park,  $\alpha$ -Galactosidase delivery using 30Kc19-human serum albumin nanoparticles for effective treatment of Fabry disease, *Appl. Microbiol. Biotechnol* 100 (2016) 10395–10402; (i) S. Jaferian, M. Soleymaninejad, B. Negahdari, A. Eatemadi, Stem cell, biomaterials and growth factors therapy for hepatocellular carcinoma, *Biomed. Pharmacother.* 88 (2017) 1046–1053. (j) M. Zhang, P. Yuan, N. Zhou, Y. Su, M. Shao, C. Chi, pH-Sensitive N-doped carbon dots–heparin and doxorubicin drug delivery system: preparation and anticancer research, *RSC Adv.* 7 (2017) 9347–9356.
- [10] J.F. Lovell, T.W. B. Liu, J. Chen, G. Zheng, Activatable photosensitizers for imaging and therapy, *Chem. Rev.* 110 (2010) 2839–2857.
- [11] J. Usuda, S. Ichinose, T. Ishizumi, H. Hayashi, K. Ohtani, S. Maehara, S. Ono, H. Honda, N. Kajiwara, O. Uchida, H. Tsutsui, T. Ohira, H. Kato, N. Ikeda, Outcome of photodynamic therapy using NPe6 for bronchogenic carcinomas in central airways >1.0 cm in diameter, *Cancer Therapy: Clinical* 16 (2010) 2198–2204.
- [12] G. Kniebühler, T. Pongratza, C. Betzb, B. Gökec, R. Srokaa, H. Steppa, J. Schirra, Photodynamic therapy for cholangiocarcinoma using low dose mTHPC (Foscan®), *Photodiagn. Photodyn.* 10 (2013) 220–228.
- [13] Y. Istomina, T. Lapzevicha, V. Chalaua, S. Shliakhtsin, T. Trukhachova, Photodynamic therapy of cervical intraepithelial neoplasia grades II and III with Photolon®, *Photodiagn. Photodyn.* 7 (2010) 144–151.
- [14] N.V. Koudinova, J.H. Pinthus, A. Brandis, O. Brenner, P. Bendel, J. Ramon, Z. Eshhar, A. Scherz, Y. Salomon, Photodynamic therapy with Pd-bacteriopheophorbide (TOOKAD):

Successful in vivo treatment of human prostatic small cell carcinoma xenografts, *Cancer Diagnosis Therapy* 104 (2003) 782–789.

[15] A.V. Reshetnickov, G.V. Ponomarev, A.V. Ivanov, O.Yu. Abakumova, T.A. Tsvetkova, A.V. Karmenyan, A.G. Rebeko, R.Ph. Baum, Novel drug form of chlorin e<sub>6</sub>, SPIE proc. optical methods for tumor treatment and detection: mechanisms and techniques in photodynamic therapy IX T.J. Dougherty ed. 3909 (2000) 124–129.

[16] E. Zenkevich, E. Sagun, V. Knyukshto, A. Shulga, A. Mironov, O. Efremova, R. Bonnett, S. Phinda Songca, M. Kassem, Photophysical and photochemical properties of potential porphyrin and chlorin photosensitizers for PDT, *J. Photochem. Photobiol. B.* 33 (1996) 171–180.

[17] E.S. Nyman, P.H. Hynninen, Research advances in the use of tetrapyrrolic photosensitizers for photodynamic therapy, *J. Photochem. Photobiol. B.* 73 (2004) 1–28.

[18] (a) D.E.J.G.J. Dolmans, D. Fukumura, R.K. Jain, Photodynamic therapy for cancer, *Nature reviews* 3 (2003) 380–387; (b) P. Agostinis, K. Berg, K. A. Cengel, T. H. Foster, A. W. Girotti, S.O. Gollnick, S.M. Hahn, M.R. Hamblin, A. Juzeniene, D. Kessel, M. Korbelik, J. Moan, P. Mroz, D. Nowis, J. Piette, B.C. Wilson, J. Golab, Photodynamic therapy of cancer: an update, *CA Cancer J. Clin.* 61 (2011) 250–281.

[19] (a) Z. Meng, B. Yu, G. Han, M. Liu, B. Shan, G. Dong, Z. Miao, N. Jia, Z. Tan, B. Li, W. Zhang, H. Zhu, C. Sheng, J. Yao, Chlorin p6-based water-soluble amino acid derivatives as potent photosensitizers for photodynamic therapy, *J. Med. Chem.* 59 (2016) 4999–5010; (b) J. M. Dabrowski, B. Pucelik, A. Regiel-Futyra, M. Brindell, O. Mazuryk, A. Kyziol, G. Stochel, W. Macyk, L.G. Arnaut, Engineering of relevant photodynamic processes through structural modifications of metallotetrapyrrolic photosensitizers, *Coord. Chem. Rev.* 325 (2016) 67–101.

[20] M. Ethirajan, Y. Chen, P. Joshi, R. K. Pandey, The role of porphyrin chemistry in tumor imaging and photodynamic therapy, *Chem. Soc. Rev.* 40 (2011) 340–362.

[21] (a) B. Yu, L.-d. Tang, Y.-l. Li, S.-h. Song, X.-l. Ji, M.-s. Lin, C.-F. Wu, Design, synthesis and antitumor activity of 4-aminoquinazoline derivatives targeting VEGFR-2 tyrosine kinase, *Bioorg. Med. Chem. Lett.* 22 (2012) 110–114; (b) Z. Song, Y. Ge, C. Wang, S. Huang, X. Shu, K. Liu, Y. Zhou, X. Ma, Challenges and perspectives on the development of small-molecule EGFR inhibitors against T790M-mediated resistance in non-small-cell lung cancer, *J. Med. Chem.* 59 (2016) 6580–6594; (c) K.N. Ganjoo, H. Wakelee, Review of erlotinib in the treatment of advanced non-small cell lung cancer, *Biologics* 1 (2007) 335–346; (d) T.P. Selvam, P.V. Kumar, Quinazoline marketed drugs – a review, *Res. Pharm.* 1 (2011) 1–21; (e) S. Dhillon, A.J. Wagstaff, Lapatinib, *Drugs* 67 (2007) 2101–2108.

[22] (a) S.A. Wells Jr, B.G. Robinson, R.F. Gagel, H. Dralle, J.A. Fagin, M. Santoro, E. Baudin, R. Elisei, B. Jarzab, J.R. Vasselli, J. Read, P. Langmuir, A.J. Ryan, M.J. Schlumberger, Vandetanib in patients with locally advanced or metastatic medullary thyroid cancer: a randomized, double-blind phase III trial, *J. Clin. Oncol.* 30 (2012) 134–141; (b) S.R. Brave, R. Odedra, N.H. James, N.R. Smith, G.B. Marshall, K.L. Acheson, D. Baker, Z. Howard, L. Jackson, K. Ratcliffe, A. Wainwright, S.C. Lovick, D.M. Hickinson, R.W. Wilkinson, S.T. Barry, G. Speake, A.J. Ryan, Vandetanib inhibits both VEGFR-2 and EGFR signalling at clinically relevant drug levels in preclinical models of human cancer, *Int. J. Oncol.* 39 (2011) 271–278; (c) H. Takeda, N. Takigawa, K. Ohashi, D. Minami, I. Kataoka, E. Ichihara, N. Ochi, M. Tanimoto, K. Kiura, Vandetanib is effective in EGFR-mutant lung cancer cells with PTEN deficiency, *Experimental Cell Research* 319 (2013) 417–423; (d) A. Levitzki, E. Mishani, Tyrosine kinases and other tyrosine kinase inhibitors, *Annu. Rev. Biochem.* 75 (2006) 93–109; (e) M.T. Conconi, G. Marzaro, L. Urbani, I. Zanusso, R.D. Liddo, I. Castagliuolo, P. Brun, F. Tonus, A. Ferrarese, A. Guiotto, A. Chilin, Quinazoline-based multi-tyrosine kinase inhibitors: synthesis, modeling, antitumor and antiangiogenic properties, *Eur. J. Med. Chem.* 67 (2013) 373–383.

- [23] A.V. Nyuchev, V.F. Otvagin, A.E. Gavryushin, Y.I. Romanenko, O.I. Koifman, D.V. Belykh, H.-G. Schmalz, A.Yu. Fedorov, Synthesis of chlorin–(arylamino)quinazoline hybrids as models for multifunctional drug development, *Synthesis* 47 (2015) 3717–3726.
- [24] T.G. Gant, S. Sarshar, M. Manoucherhr, WO 2010/028254 A2.
- [25] (a) H. Tamiaki, S. Takeuchi, S. Tsudzuki, T. Miyatake, R. Tanikaga, Self-aggregation of synthetic zinc chlorins with a chiral 1-hydroxyethyl group as a model for *in vivo* epimeric bacteriochlorophyll-c and d aggregates, *Tetrahedron* 54 (1998) 6699–6718.
- [26] A. El-Faham, F. Albericio, Peptide coupling reagents, more than a letter soup, *Chem. Rev.* 111 (2011) 6557–6602.
- [27] D.V. Belykh, E.A. Kopylov, I.V. Gruzdev, A.V. Kuchin, Opening of the extra ring in pheophorbide a methyl ester by the action of amines as a one-step method for introduction of additional fragments at the periphery of chlorin macroring, *Russ. J. Org. Chem.* 46 (2010) 577–585.
- [28] P.S. Donnelly, S.D. Zanatta, S.C. Zammit, J.M. White, S.J. Williams, ‘Click’ cycloaddition catalysts: copper(I) and copper(II) tris(triazolylmethyl)amine complexes, *Chem. Commun.* 0 (2008) 2459–2461.
- [29] D.V. Belykh, I.S. Tarabukina, I.V. Gruzdev, M.I. Kodess, A.V. Kutchina, Aminomethylation of chlorophyll a derivatives using bis(N,N-dimethylamino)methane, *J. Porphyr. Phthalocyan.* 13 (2009) 949–956.
- [30] (a) J. Ferreira, P.F.C. Menezes, C. Kurachi, C. Sibata, R.R. Allison, V.S. Bagnato, Photostability of different chlorin photosensitizers, *Laser Phys. Lett.* 5 (2008) 156–161; (b) B. Ormond, H.S. Freeman, Dye sensitizers for photodynamic therapy, *Materials* 6 (2013) 817–840.
- [31] A.H. Colagar, O. Amjadi, R. Valadan, A. Rafiei, Minimal HER1 and HER2 expressions in CHO and HEK-293 cells cause them appropriate negative cells for HERs-related studies. *Res. Mol. Med.* 1 (2013) 6–12.

- [32] (a) F. Zhang, S. Wang, L. Yin, Y. Yang, Y. Guan, W. Wang, H. Xu, N. Tao, Quantification of epidermal growth factor receptor expression level and binding kinetics on cell surfaces by surface plasmon resonance, *Anal. Chem.* 87 (2015) 9960–9965; (b) M. Eiblmaier, L.A. Meyer, M.A. Watson, P.M. Fracasso, L.J. Pike, C.J. Anderson, Correlating EGFR expression with receptor-binding properties and internalization of  $^{64}\text{Cu}$ -DOTA-cetuximab in 5 cervical cancer cell lines, *J. Nucl. Med.* 49 (2008) 1472–1479.
- [33] P. Stanton, S. Richards, J. Reeves, M. Nikolic, K. Edington, L. Clark, G. Robertson, D. Souter, R. Mitchell, F.J. Hendler, Epidermal growth factor receptor expression by human squamous cell carcinomas of the head and neck, cell lines and xenografts, *Br. J. Cancer* 70 (1994) 427–433.
- [34] For A431 cell line see: (a) E.J. Cho, J. Yang, K.A. Mohamedali, E.K. Lim, E.J. Kim, C.J. Farhangfar, J.S. Suh, S. Haam, M.G. Rosenblum, Y.M. Huh, Sensitive angiogenesis imaging of orthotopic bladder tumors in mice using a selective magnetic resonance imaging contrast agent containing VEGF121/rGel, *Invest. Radiol.* 46 (2011) 441–449; for HeLa cell line see: (b) B. Das, H. Yeger, R. Tsuchida, R. Torkin, M.F. Gee, P.S. Thorner, M. Shibuya, D. Malkin, S. Baruchel, A hypoxia-driven vascular endothelial growth factor/Flt1 autocrine loop interacts with hypoxia-inducible factor-1A through mitogen-activated protein kinase/extracellular signal-regulated kinase 1/2 pathway in neuroblastoma, *Cancer Res.* 65 (2005) 7267–7275; (c) T. Takahashi, S. Yamaguchi, K. Chida, M. Shibuya, A single autophosphorylation site on KDR/Flk-1 is essential for VEGF-A-dependent activation of PLC- $\gamma$  and DNA synthesis in vascular endothelial cells, *EMBO J.* 20 (2001) 2768–2778. For CHO cell line see: (d) P. Farnia, M. Bandehpour, J. Ghanavi, B. Kazemi, Cloning and expression of soluble vascular endothelial growth factors receptor-1 (sFlt-1) fragments in CHO-K1, *Int. J. Clin. Exp. Med.* 6 (2013) 773–778.
- [35] H.J. Jones, D.J. Veron, S.B. Brown, Photodynamic therapy effect of m-THPC (Foscan®) *in vivo*: correlation with pharmacokinetics, *Cancer Res. UK.* 89 (2003) 398–404.

- [36] (a) A.M. Ronn, J. Batti, C.J. Lee, D. Yoo, M.E. Siegel, M. Nouri, L.A. Lofgren, B.M. Steinberg, Comparative biodistribution of meta-tetra(hydroxyphenyl) chlorin in multiple species: clinical implications for photodynamic therapy, *Lasers Surg. Med.* 20 (1997) 437–442. (b) T. McCaffrey, A.K. D'Cruz, M. Biel, Effect of tumor depth and surface illumination on tumor response in patients treated with Foscan-mediated photodynamic therapy (PDT), *Proc. Am. Soc. Clin. Oncol* 22 (2003) 503.
- [37] M.R. Wasielewski, W.A. Svec, Synthesis of covalently linked dimeric derivatives of chlorophyll a, pyrochlorophyll a, chlorophyll b, and bacteriochlorophyll a, *J. Org. Chem.* 45 (1980) 1969–1674.
- [38] T. Mosmann, Rapid colorimetric assay for cellular growth and survival: application to proliferation and cytotoxicity assays, *J. Immunol. Methods* 65 (1983) 55–63.
- [39] N.Y. Shilyagina, V.I. Plekhanov, I.V. Shkunov, P.A. Shilyagin, L.V. Dubasova, A.A. Brilkina, E.A. Sokolova, I.V. Turchin, I.V. Balalaeva, LED light source for *in vitro* study of photosensitizing agents for photodynamic therapy, *Sovremennye Tehnologii v Medicine* 6 (2014) 15–22.

**Highlights:**

- A novel water-soluble chlorin-(arylamino)quinazoline conjugate was synthesized.
- The conjugate exhibited selective accumulation in cells with high level of EGFR expression.
- A pronounced  $IC_{50\text{dark}}/IC_{50\text{light}}$  ratio has been achieved.
- The conjugate preferably accumulated in the tumor tissue of tumor-bearing mice.